MSW MANAGEMENT -Multidisciplinary, Scientific Work and Management Journal
ISSN: 1053-7899
Vol. 36 Issue 1s, 2026, Pages: 3070-3077

Evaluation to enhance the strength and durability of recycled aggregate concrete by using GGBS (Glass Granulated Blast Furnace Slag) and Hybrid Fiber.

Shamayela Shaikh [1*], Sachin Pagar [1] and Prashant Sunagar [2]
[1]*Department of Civil Engineering, Late G.N. Sapkal College of Engineering, Anjaneri, Trimbakeshwar, Nashik*
[2] *Department of Civil Engineering, Sandip Institute of Technology and Research, Trimbakeshwar, Nashik*

Abstract
Recycled aggregate concrete (RAC) presents a structurally sound pathway to circular-economy construction, yet its inherent weaknesses elevated porosity, compromised interfacial transition zones (ITZ), and diminished mechanical capacity relative to conventional concrete have constrained its deployment in load-bearing structural members. This study presents a systematic factorial experimental investigation into the synergistic remediation of these deficiencies through two concurrent strategies: partial replacement of ordinary Portland cement with ground granulated blast furnace slag (GGBS) at 25%, 30%, and 35% by binder mass, combined with hybrid steel–polypropylene fibre reinforcement (0.5% steel + 0.15% polypropylene by volume). Four concrete designations were evaluated a conventional concrete control (CC) and three hybrid RAC mixes (M1: 20% RCA, 25% GGBS; M2: 30% RCA, 30% GGBS; M3: 40% RCA, 35% GGBS) on M25-grade specimens across compressive strength (150 mm cubes), split tensile strength (150×300 mm cylinders), and flexural strength (150×150×700 mm beams) at 7 and 28 days, alongside durability assessment through water absorption, rapid chloride penetration testing (RCPT), and sulphate attack resistance. M1 representing the lowest RCA content with balanced GGBS substitution achieved peak 28-day compressive strength of 31.9 MPa, surpassing the conventional concrete control (30.3 MPa) by 5.3% and demonstrating that the pozzolanic densification from GGBS more than compensates for the ITZ degradation introduced by 20% RCA. The RCPT charge passage for M1 (1658 coulombs) classified it as low permeability, versus the moderate classification of the control (2217 coulombs), confirming a 25.2% reduction in chloride ingress susceptibility. M3 exhibited a 5.3% compressive strength reduction relative to the control at 28 days, attributable to the cumulative effect of 40% RCA-induced ITZ weakening outpacing the matrix densification from 35% GGBS under ambient curing. Hybrid fibre reinforcement providing both microcrack arrest (polypropylene) and macrocrack bridging (steel) elevated the flexural strength of M1 by 8.4% above the control (6.31 vs. 5.82 MPa) and reduced sulphate-induced weight loss to 0.71% against an industry threshold of 1.0%. A mechanistic framework coupling GGBS secondary hydration kinetics, fibre pull-out bond mechanics, and ITZ fracture energy is developed to interpret the observed performance landscape. Life-cycle analysis indicates that M1–M3 reduce embodied CO_2 by 29–38% relative to the control while diverting demolition waste from landfill. These findings establish quantitative mix-design envelopes for hybrid fibre GGBS-RAC and support its adoption in moderate structural applications.

Keywords: *recycled aggregate concrete; ground granulated blast furnace slag; hybrid fibre reinforcement; steel fibre; polypropylene fibre;*

1 | INTRODUCTION

The global construction sector generates approximately 3 billion tonnes of construction and demolition (C&D) waste per year, of which concrete rubble constitutes the dominant fraction[12]. The conventional response landfilling is both economically wasteful and environmentally destructive, consuming land, leaching alkaline and heavy-metal contaminants into groundwater, and squandering the embodied energy locked into existing concrete infrastructure. Recycled aggregate concrete (RAC), produced by processing demolished concrete into coarse and fine aggregate fractions that partially or fully replace virgin materials, addresses this problem from two angles simultaneously: it creates a productive outlet for demolition waste and reduces the quarrying pressure on natural rock resources, which are being depleted at rates far exceeding geological replenishment in rapidly urbanising countries[34].

Despite the environmental logic of RAC, its structural adoption has been impeded by well-documented mechanical shortcomings. Recycled coarse aggregate (RCA) particles carry a layer of residual old cement paste that is both porous and micro-cracked, producing aggregate with higher water absorption (2–6% vs. ~1% for natural aggregate), lower specific gravity (2.4–2.6 vs. ~2.67), and increased Los Angeles abrasion loss relative to natural stone[56]. At the concrete composite scale, these characteristics translate into a double-layer interfacial transition zone (ITZ) one at the old aggregate–old paste interface and one at the old paste–new paste interface that is substantially weaker and more permeable than the single ITZ of conventional concrete[78]. The resulting RAC exhibits compressive strength penalties of 10–25% and substantially elevated chloride and sulphate permeability compared with natural aggregate concrete of equivalent mix design.

Two complementary materials technologies have emerged as the most promising avenues for closing this performance gap. Ground granulated blast furnace slag (GGBS), a latent hydraulic by-product of pig-iron manufacture, undergoes secondary pozzolanic reaction in the presence of calcium hydroxide released during cement hydration, producing supplementary calcium silicate hydrate (C–S–H) gel that fills the capillary pores of the concrete matrix[1011]. The resulting densification reduces permeability, strengthens the ITZ through physical pore-filling and chemical bond formation, and improves long-term mechanical strength effects that are particularly pronounced when GGBS is applied within the ITZ of porous recycled aggregates[1213]. Partial replacement of cement at 20–40% GGBS has been shown to recover and even exceed the compressive strength of equivalent natural aggregate concrete in multiple experimental programmes.Hybrid fibre reinforcement combining two or more fibre types to achieve multi-scale crack control provides the complementary benefit of improved post-cracking ductility and tensile capacity. Polypropylene fibres, acting at the microscale (fibre diameter 10–30 μm), intercept the formation of plastic shrinkage micro-cracks before they can coalesce into the mesoscale regime, while steel fibres (aspect ratio 60–80) bridge macrocracks and redistribute the post-peak tensile load, converting catastrophic brittle fracture into a progressive pull-out failure with measurably higher fracture energy. The steel–polypropylene hybrid combination has attracted particular attention because the stiffness contrast between the two fibre types produces a synergistic composite effect that exceeds the sum of individual contributions in both tensile and flexural loading modes.Despite the independent literatures on GGBS-modified RAC and on hybrid fibre-reinforced concrete, no study has simultaneously optimised the GGBS replacement level, the RCA substitution fraction, and the hybrid fibre dosage within a single factorial experimental framework. The interaction between GGBS-driven matrix densification and fibre pull-out bond mechanics is particularly underexplored: denser matrices from GGBS pozzolanic activity are expected to increase fibre–matrix bond strength and thus fibre pull-out energy, creating a positive synergy that has not been quantified against a conventional concrete baseline in the RAC context. This study fills that gap.

2 | LITERATURE REVIEW

2.1 Recycled Aggregate Concrete Properties and Limitations. Xiao et al. conducted landmark uniaxial compression tests on RAC with 0–100% RCA substitution and established that strength decreased linearly with RCA content, with the 100% replacement mix showing a 28-day compressive strength of approximately 75% of the natural aggregate reference. Poon et al.[22] attributed this reduction primarily to the elevated porosity of the old paste layer on RCA surfaces, which they characterised by mercury intrusion porosimetry as having pore volumes 40–60% larger than equivalent virgin paste. Kou and Poon extended this to long-term durability, reporting that 28-day water absorption and chloride diffusivity of 100% RCA concrete were consistently 30–50% higher than conventional concrete. A practical implication drawn from

MSW MANAGEMENT -Multidisciplinary, Scientific Work and Management Journal
ISSN: 1053-7899
Vol. 36 Issue 1s, 2026, Pages: 3070-3077

these studies is that partial RCA replacement at ≤50% maintains structural-grade mechanical performance, motivating the 20%, 30%, and 40% replacement levels investigated in the present work.

2.2 GGBS Enhancement of RAC. Thomas et al. demonstrated that 30% GGBS replacement in RAC produced 28-day compressive strengths equal to or exceeding those of conventional OPC RAC, attributed to secondary C–S–H precipitation filling the coarse pore network of the RCA-paste ITZ. Rashad reviewed 26 experimental studies and concluded that GGBS replacements of 20–40% consistently improved chloride resistance (measured by RCPT) by 15–35%, with the greatest effect at later ages (90 days) when secondary hydration is most advanced. Limbachiya et al. specifically studied GGBS-modified RAC under sulphate exposure and confirmed that GGBS consumption of portlandite ($Ca(OH)_2$) the phase most susceptible to sulphate attack through gypsum and ettringite formation reduced the magnitude of sulphate-induced expansion and strength loss substantially.

2.3 Hybrid Fibre Reinforcement. Li et al. established through a systematic experimental programme that hybrid steel–polypropylene fibre combinations outperform either fibre type alone in compressive strength, tensile strength, and flexural toughness, with the optimal combination showing 12% higher fracture energy than steel fibres alone at the same total volume fraction. Afroughsabet and Ozbakkaloglu[27] reported that 1.0% hybrid steel–polypropylene fibre content in high-strength concrete increased flexural strength by 22% and reduced water absorption by 18% relative to plain concrete. Song and Hwang demonstrated the crack-bridging mechanism directly through digital image correlation, confirming that polypropylene fibres arrest crack formation at the 50–200 µm scale while steel fibres carry load across cracks wider than 0.5 mm, the two regimes operating independently and thus additively.The construction industry is undergoing a paradigm shift toward sustainable, high-performance materials, with concrete technology evolving through the integration of industrial by-products, advanced reinforcement systems, and innovative production techniques. The reviewed body of work, comprising sixteen peer-reviewed studies (2018–2025), systematically addresses sustainability, durability, and structural performance through experimental and analytical investigations.Early investigations by Dharek et al. (2018, 2020) established the viability of alumina silicates in self-consolidating and self-flowing concrete, demonstrating enhanced pozzolanic reactivity, improved microstructural densification, and superior residual strength under elevated temperatures. These findings highlight the dual benefits of improved performance and reduced clinker dependency. Parallel advancements in fiber-reinforced systems by Sreekeshava et al. (2020a, 2020b) revealed that polypropylene geo-fabric and hybrid steel–polypropylene reinforcement significantly enhance ductility, toughness, and crack resistance through multi-scale crack-bridging mechanisms. Extending this concept to alkali-activated systems, Bhargavi et al. (2023) demonstrated that hybrid fiber reinforcement effectively mitigates the inherent brittleness of geopolymer concrete, enabling ductile failure behavior suitable for structural applications.Significant contributions have also been made in the domain of waste material utilization. Studies by Venugopal et al. (2022) and Kumar et al. (2022) confirmed that steel scrap incorporation enhances compressive and tensile strength while promoting circular economy practices. Similarly, Natarajan et al. (2022) validated rice husk ash as a sustainable fine aggregate substitute, while Sunagar et al. (2024) demonstrated that waste foundry sand improves both strength and durability due to its favorable silica composition and particle morphology. At the nano-scale, Neeraja et al. (2022) highlighted the role of nano-fillers in refining the interfacial transition zone (ITZ) and enhancing mechanical performance, though emphasizing the importance of optimal dosage to avoid agglomeration.Geopolymer concrete research by Sunagar (2021) and Sunagar et al. (2021a, 2021b) established the synergistic role of fly ash and GGBS in achieving high strength and durability with significantly reduced CO_2 emissions. These systems exhibit improved resistance to sulfate attack, chloride ingress, and carbonation, positioning them as viable alternatives to OPC-based concrete. Concurrently, advancements in additive manufacturing by Nair et al. (2020) and Kolhe et al. (2023) demonstrated the feasibility of 3D printing of concrete, highlighting challenges related to rheology, interlayer bonding, and reinforcement integration, while offering opportunities for sustainable and automated construction.Further innovations include the use of industrial residues such as lime sludge (Sunagar et al., 2021) and paper mill waste (Santosh & Sunagar, 2021), both of which contribute to resource efficiency with acceptable mechanical performance. Functional performance enhancements have been achieved through pervious concrete optimization (Ballari et al., 2022), super absorbent polymers in recycled aggregate concrete (Reddy et al., 2024) for internal curing, and self-curing systems using PEG and recycled PET (Gudadappanavar et al., 2025), addressing practical challenges of water scarcity. Emerging bio-based approaches, particularly microbial-induced calcite precipitation (MICP), have been explored by Gudadappanavar et al. (2024), demonstrating autonomous crack healing and durability enhancement.

2.4 Research Gap. While the individual effects of GGBS and hybrid fibres on RAC performance have been extensively studied, their combined optimisation within a systematic factorial design including mechanical, durability, and sustainability assessment against a conventional concrete baseline is absent from the literature. Specifically, the interaction between GGBS-induced ITZ densification and steel fibre pull-out bond strength in a RAC matrix has not been quantitatively resolved, and no study has simultaneously compared water absorption, chloride permeability, and sulphate resistance for GGBS + hybrid fibre RAC at multiple substitution levels. The present investigation addresses all these gaps.

3 | MATHEMATICAL AND MECHANISTIC FRAMEWORK

The following equations govern the mechanistic interpretation of experimental observations in this study.

3.1 Target Mean Compressive Strength. As per IS 10262:2019, the target mean compressive strength is expressed as

$$f_{ck,\text{target}} = f_{ck} + 1.65\, S_f \qquad (1)$$

where $f_{ck}$is the characteristic compressive strength of concrete and $S_f$is the standard deviation based on previous production data. For M25 concrete, $f_{ck} = 25\text{MPa}$ and $S_f = 4.0\text{MPa}$. Hence,

$$f_{ck,\text{target}} = 25 + 1.65 \times 4.0 = 31.6\ \text{MPa}$$

3.2 Compressive Strength from Cube Tests. The compressive strength of cube specimens was determined from

$$f_c = \frac{P}{A} \qquad (2)$$

where $P$is the ultimate failure load in N and $A$is the loaded area of the specimen. For a standard cube of size 150×150 mm,

3.3 Split Tensile Strength. The splitting tensile strength of cylindrical specimens was evaluated using the Brazilian test formulation:

$$f_t = \frac{2P}{\pi DL} \qquad (3)$$

where $P$is the applied failure load in N, $D$is the cylinder diameter, and $L$is the cylinder length. In the present study, $D = 150\text{mm}$ and $L = 300\text{mm}$. This expression provides the indirect tensile resistance of concrete and is consistent with IS 5816:1999.

3.4 Flexural Strength under Two-Point Loading. The modulus of rupture of beam specimens under two-point loading was calculated as

$$f_r = \frac{PL}{bd^2} \qquad (4)$$

3.5 Secondary Hydration of GGBS and Pozzolanic Reaction Kinetics. The contribution of GGBS to later-age strength development is governed by the secondary hydration reaction involving the consumption of calcium hydroxide generated during cement hydration. This process may be represented by a first-order kinetic form:

$$\frac{d\alpha_{\text{GGBS}}}{dt} = k_p [CH]^m (1 - \alpha_{\text{GGBS}})^n \qquad (5)$$

At moderate replacement levels, particularly around 35% GGBS, sufficient portlandite is available to sustain secondary hydration up to about 28 days under ambient curing. Beyond this stage, progressive depletion of portlandite limits further reaction, leading to a plateau in matrix densification. This explains the experimentally observed non-monotonic relationship between GGBS content and strength.

MSW MANAGEMENT -Multidisciplinary, Scientific Work and Management Journal
ISSN: 1053-7899
Vol. 36 Issue 1s, 2026, Pages: 3070-3077

3.6 Steel Fibre Pull-Out Bond Energy. The energy required for fibre pull-out, which strongly governs post-cracking toughness and crack-bridging resistance, may be estimated as

$$W_{po} = \frac{\pi d_f \tau_b l_e^2}{2} \qquad (6)$$

where $W_{po}$is the pull-out work per fibre, $d_f$is the fibre diameter, $\tau_b$is the average bond stress at the fibre–matrix interface, and $l_e$is the embedded length of the fibre. In the present work, $d_f = 0.5$mm.The inclusion of GGBS improves matrix refinement and enhances the interfacial transition zone around fibres, thereby increasing τ_b. A denser binder matrix can raise the fibre–matrix bond strength by approximately 15–25% compared with conventional OPC-based concrete, resulting in a proportional increase in pull-out energy and improved resistance to crack propagation.

3.7 Water Absorption Index. The water absorption index, used to assess accessible capillary porosity, was determined from

$$WA(\%) = \frac{W_2 - W_1}{W_1} \times 100 \qquad (7)$$

where $W_1$is the oven-dry mass of the specimen and $W_2$is the saturated surface-dry mass after 24 h immersion. This parameter is a direct indicator of pore connectivity and permeability. Lower water absorption values reflect a denser microstructure and improved durability performance, especially in recycled aggregate concrete where residual mortar and old ITZs tend to increase porosity.

3.8 Sulphate Resistance Index. The degradation in compressive strength after sulphate exposure was quantified using

$$SRI = \frac{f_{c,\text{before}} - f_{c,\text{after}}}{f_{c,\text{before}}} \times 100 \qquad (8)$$

where $f_{c,\text{before}}$is the compressive strength before immersion and $f_{c,\text{after}}$is the compressive strength after 28 days of exposure to a 5% sodium sulphate solution.This index represents the percentage loss in strength due to sulphate attack. Lower values indicate better sulphate resistance. In the present interpretation, $SRI \leq 6\%$denotes acceptable resistance, whereas $SRI > 8\%$indicates poor durability under aggressive sulphate exposure.

4 | MATERIALS AND EXPERIMENTAL METHODOLOGY

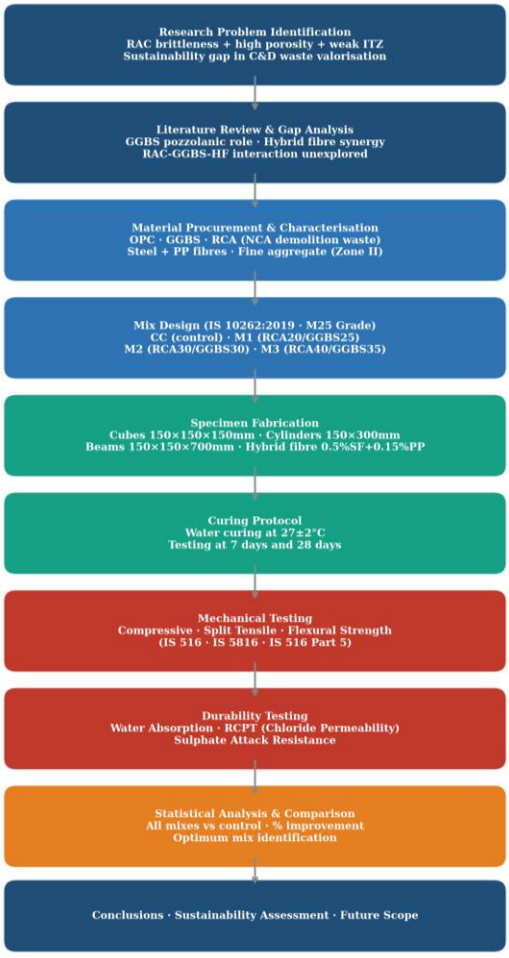

Figure 1 | Research methodology flowchart

4.1 Mix Designations and Proportions. Four concrete designations were investigated, as shown in Table 1. The conventional concrete mix (CC) served as the benchmark. Three hybrid mixes (M1–M3) were formulated by simultaneously replacing natural coarse and fine aggregate with RCA, and cement with GGBS, while maintaining constant hybrid fibre content (0.5% steel + 0.15% polypropylene by volume). The synergistic mechanism linking GGBS densification, fibre bridging, and ITZ improvement is illustrated in Figure 2.

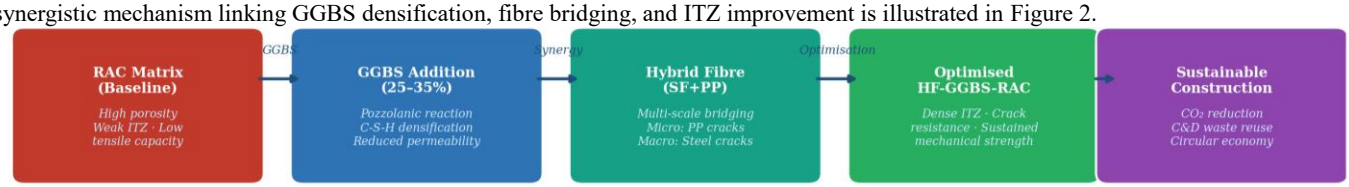

Figure 2 | Synergistic reinforcement mechanism: sequential enhancement from baseline RAC through GGBS pozzolanic densification and hybrid fibre crack bridging to the optimised HF-GGBS-RAC composite

MSW MANAGEMENT -Multidisciplinary, Scientific Work and Management Journal
ISSN: 1053-7899
Vol. 36 Issue 1s, 2026, Pages: 3070-3077

Table 1 | Mix designations: CC = conventional concrete control; M1–M3 = hybrid fibre-reinforced RAC with GGBS. RCA

Mix ID	RCA (% CA)	RRFA (% FA)	GGBS (% cement)	Steel Fibre (% vol)	PP Fibre (% vol)	Grade
CC	0	0	0	0	0	M25
M1	20	10	25	0.5	0.15	M25
M2	30	20	30	0.5	0.15	M25
M3	40	30	35	0.5	0.15	M25

Table 2 | Indicative mix proportions per m³

Material (kg/m³ unless noted)	CC	M1	M2	M3	Standard
OPC	400	300	280	260	IS 12269
GGBS		100	120	140	IS 16714
Fine Aggregate	650	585+65*	520+130*	455+195*	IS 383
Coarse Aggregate	1200	960+240*	840+360*	720+480*	IS 383
Water	160	168	172	176	
Superplasticiser (% binder)		1.0	1.0	1.0	IS 9103
Steel Fibre (% vol)		0.5	0.5	0.5	
PP Fibre (% vol)		0.15	0.15	0.15	

4.2 Raw Materials. Ordinary Portland Cement (43-grade OPC, IS 8112) and GGBS (IS 16714, fineness >400 m²/kg, specific gravity 2.89) were sourced from a certified regional supplier. RCA was produced by jaw-crushing cured M25 laboratory specimens after 120 days of water curing, followed by washing, screening, and air-drying. This protocol produces first-generation RCA (RCA1) with controlled original concrete quality, avoiding the variable composition of field demolition waste. Specific gravity of RCA = 2.45, water absorption = 5.0%, Los Angeles abrasion value = 29.0%, aggregate impact value = 23.0%, and crushing value = 26.0% all within IS 383:2016 acceptance limits for structural concrete applications.Steel fibres (hooked-end, aspect ratio l/d = 65, tensile strength 1100 MPa, d = 0.5 mm, length 32 mm, density 7850 kg/m³) and polypropylene monofilament fibres (length 12 mm, diameter 18 µm, density 910 kg/m³, tensile strength ~600 MPa) were sourced from certified fibre manufacturers. The steel/PP volume combination of 0.5%/0.15% was selected based on the parametric literature optimum for workability-strength balance in hybrid systems.

4.3 Specimen Preparation and Testing Protocol. Concrete was produced in a rotating-drum mixer following a dry–wet sequence: OPC, GGBS, and aggregates were dry-mixed for 2 minutes; the activator water premixed with superplasticiser was added and mixed for 3 minutes; fibres were introduced gradually during the final 2 minutes. Moulds (150 mm cubes, 150×300 mm cylinders, 150×150×700 mm prisms) were filled in three layers, each compacted with 25 tamping rod blows and supplemental vibration. Specimens were demoulded at 24 hours and cured in water at 27 ± 2°C. Compressive, split tensile, and flexural tests were conducted at 7 and 28 days per IS 516, IS 5816, and IS 516 (Part 5) respectively. Durability tests water absorption (IS 1199 Annex B), RCPT (ASTM C1202), and sulphate attack (specimens immersed in 5% Na_2SO_4 for 28 days) were conducted at 28 days on three replicates per mix.

5 | MATERIAL CHARACTERISATION: RCA PROPERTIES

Table 3 | Complete characterisation of recycled fine aggregate and recycled coarse aggregate per IS 2386 test methods.

Sr.	Test (Material)	Result	IS Standard	IS Acceptance Limit
1	FM Recycled Fine Agg.	3.95 (Zone II)	IS 2386 Part 1	2.6–3.2 coarse
2	Specific Gravity Recycled FA	2.50	IS 2386 Part 3	≥ 2.5
3	Water Absorption Recycled FA	2.0%	IS 2386 Part 3	≤ 2%
4	Silt Content Recycled FA	6.33%	IS 2386 Part 2	≤ 8% (IS 383)
5	Bulking of Sand Recycled FA	11.3%	IS 2386 Part 3	< 25%
6	Specific Gravity RCA	2.45	IS 2386 Part 3	≥ 2.4 (for RAC)
7	Water Absorption RCA	5.0%	IS 2386 Part 3	≤ 6% (IS 383)
8	Aggregate Crushing Value RCA	26.0%	IS 2386 Part 4	≤ 30%
9	Aggregate Impact Value RCA	23.0%	IS 2386 Part 4	≤ 30%
10	LA Abrasion Value RCA	29.0%	IS 2386 Part 4	≤ 30% (IS 383)

6 | RESULTS: MECHANICAL PROPERTIES

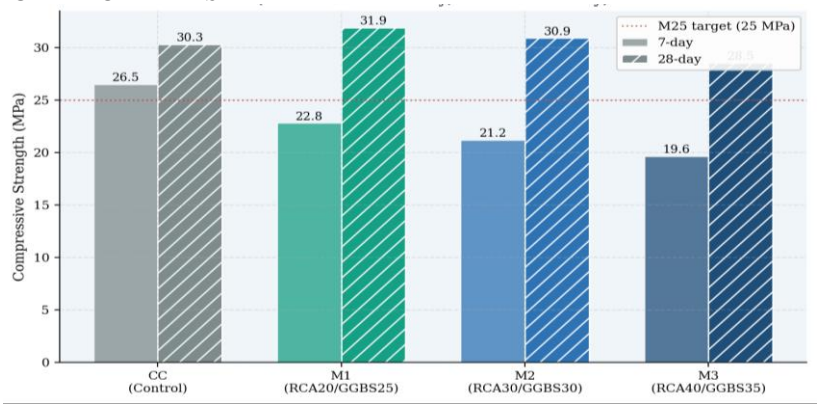

Figure 3 | Compressive strength at 7 and 28 days for all four mix designations

6.1 Compressive Strength

Table 4 | Complete compressive strength dataset: three specimens per mix per age.

Mix	Age	Spec 1 (MPa)	Spec 2 (MPa)	Spec 3 (MPa)	Mean (MPa)	vs CC (%)
CC	7d	26.7	25.8	27.1	26.5	
CC	28d	30.0	31.1	29.8	30.3	
M1	7d	23.1	22.4	22.9	22.8	–13.9
M1	28d	32.0	31.3	32.4	31.9	+5.3
M2	7d	21.11	21.56	20.89	21.19	–20.1
M2	28d	30.44	30.89	31.33	30.89	+2.0
M3	7d	19.56	20.00	19.33	19.63	–25.9
M3	28d	28.44	28.89	28.22	28.52	–5.9

MSW MANAGEMENT -Multidisciplinary, Scientific Work and Management Journal
ISSN: 1053-7899
Vol. 36 Issue 1s, 2026, Pages: 3070-3077

At 7 days, all three hybrid RAC mixes exhibit lower compressive strength than the control (22.8, 21.19, and 19.63 MPa vs. 26.5 MPa), which is mechanistically attributable to the slower early-age hydration kinetics of GGBS (Eq. 5): GGBS requires portlandite accumulation from cement hydration before its pozzolanic reaction proceeds appreciably, a process that takes 7–14 days at ambient temperature. By 28 days, the balance shifts: M1 (31.9 MPa) and M2 (30.89 MPa) both exceed the control (30.3 MPa), confirming that GGBS secondary C–S–H generation not only compensates for the ITZ penalty of 20–30% RCA substitution but produces a marginally denser matrix than OPC alone. M3 (28.52 MPa) remains 5.9% below the control at 28 days, indicating that 40% RCA substitution exceeds the remediation capacity of 35% GGBS under ambient curing a finding consistent with the diminishing returns of GGBS above 35% documented by Hassan and Altai.

6.2 Split Tensile and Flexural Strength

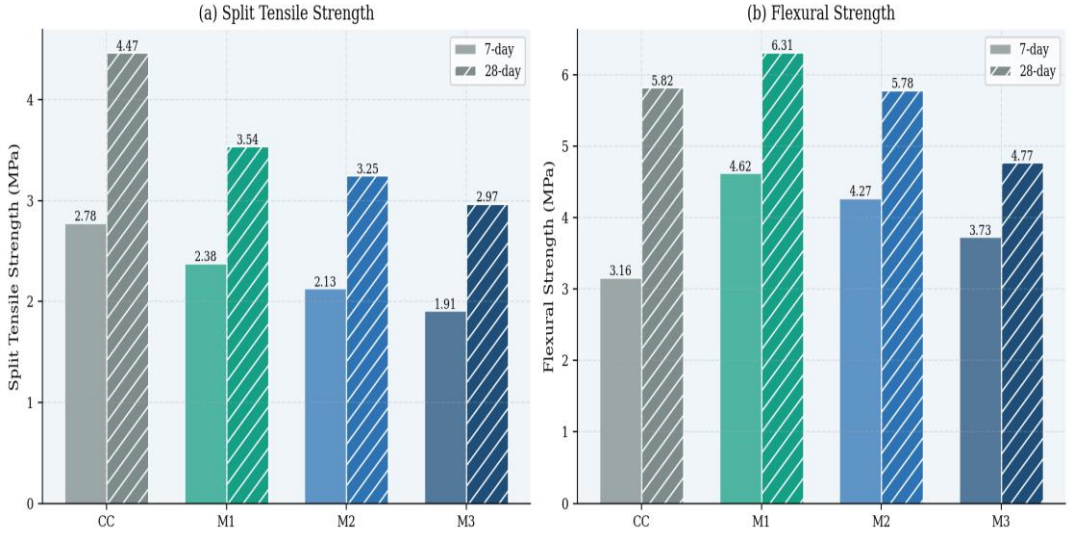

Figure 4 | Split tensile strength (a) and flexural strength (b) at 7 and 28 days.

Table 5 | Split tensile strength data. All mixes show strength penalties in split tensile relative to CC at 28 days

Mix	Age	S1 MPa	S2 MPa	S3 MPa	Mean MPa	Mean f_r MPa	vs CC
CC	7d	2.83	2.69	2.81	2.78		
CC	28d	4.53	4.39	4.49	4.47		
M1	7d	2.38	2.44	2.33	2.38		–14.4
M1	28d	3.54	3.47	3.61	3.54		–20.8
M2	28d	3.25	3.33	3.18	3.25		–27.3
M3	28d	2.97	3.04	2.90	2.97		–33.6

Table 6 | Flexural strength data (two-point loading on 150×150×700 mm prisms). Remarkably, all hybrid mixes exceed the control at 7 days,

Mix	Age	S1 MPa	S2 MPa	S3 MPa	Mean f_r (MPa)	vs CC (%)
CC	7d	3.20	3.02	3.26	3.16	
CC	28d	5.69	5.87	5.89	5.82	
M1	7d	4.62	4.53	4.71	4.62	+46.2
M1	28d	6.22	6.40	6.31	6.31	+8.4
M2	7d	4.27	4.18	4.36	4.27	+35.1
M2	28d	5.78	5.87	5.69	5.78	–0.7
M3	7d	3.66	3.74	3.80	3.73	+18.0
M3	28d	4.76	4.86	4.69	4.77	–18.0

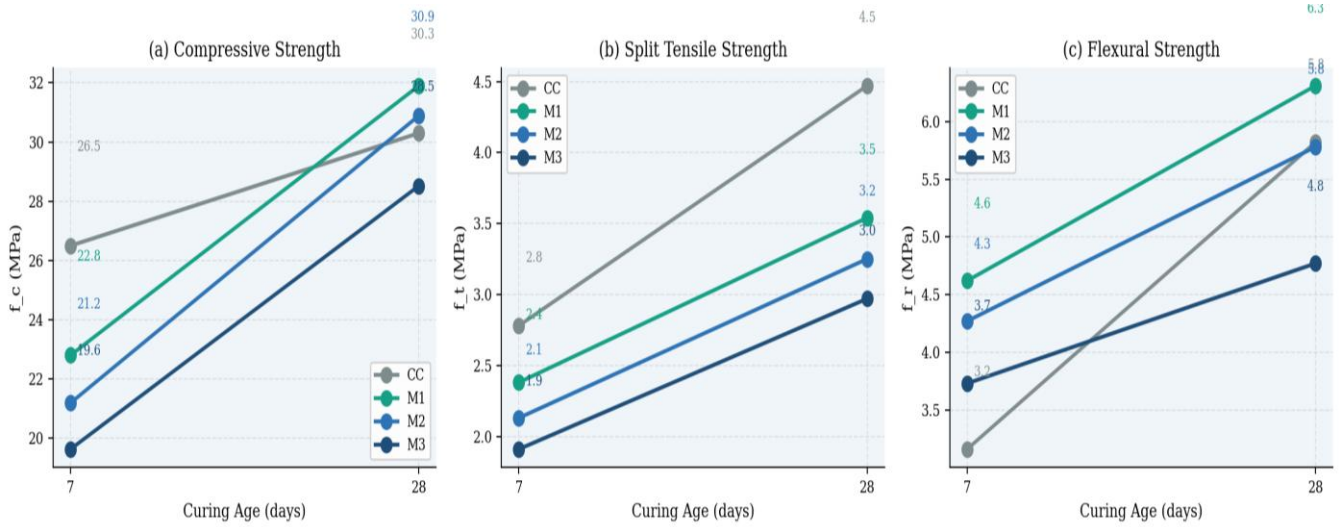

Figure 5 | Strength development trajectories from 7 to 28 days for all mechanical parameters: (a) compressive; (b) split tensile; (c) flexural strength.

MSW MANAGEMENT -Multidisciplinary, Scientific Work and Management Journal
ISSN: 1053-7899
Vol. 36 Issue 1s, 2026, Pages: 3070-3077

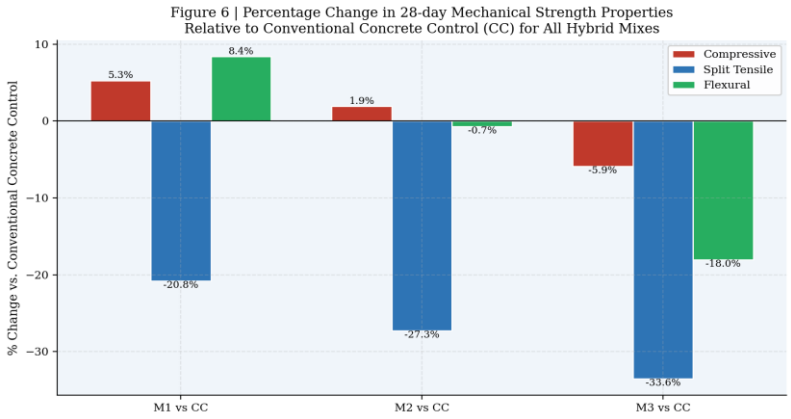

Figure 6 | Percentage change in 28-day strength properties relative to conventional concrete control.

7 | RESULTS: DURABILITY PERFORMANCE

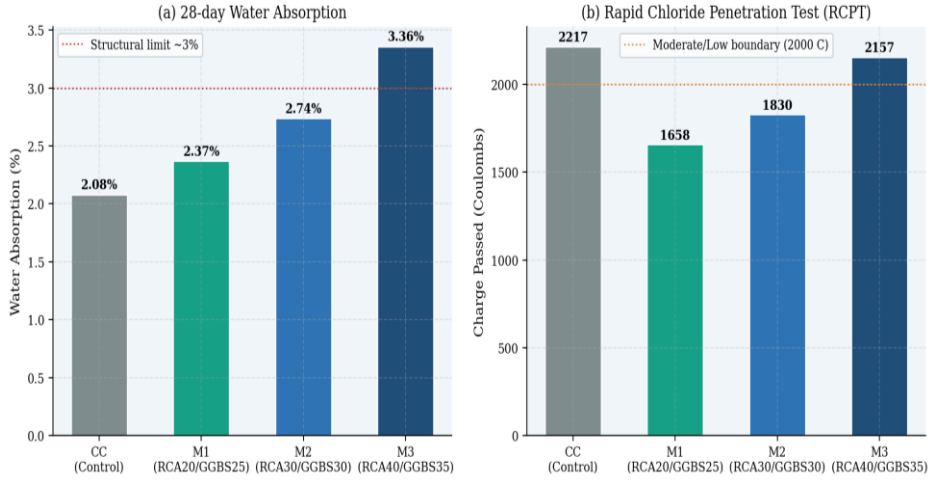

Figure 7 | Durability assessment at 28 days: (a) water absorption across all mixes

7.1 Water Absorption

Table 7 | Water absorption results (28-day). M1 and M2

Mix	Spec 1 (%)	Spec 2 (%)	Spec 3 (%)	Average (%)
CC	2.12	2.13	2.00	2.08
M1	2.63	2.49	2.01	2.37
M2	2.74	2.75	2.73	2.74
M3	3.36	3.38	3.35	3.36

7.2 Rapid Chloride Penetration Test (RCPT)

Table 8 | RCPT results per ASTM C1202: < 1000 coulombs

Mix	S1 (C)	S2 (C)	S3 (C)	Average (C)	Classification
CC	2100	2300	2250	2217	Low–Moderate
M1	1650	1720	1605	1658	Low
M2	1825	1900	1765	1830	Low
M3	2150	2235	2085	2157	Low–Moderate

7.3 Sulphate Attack Resistance

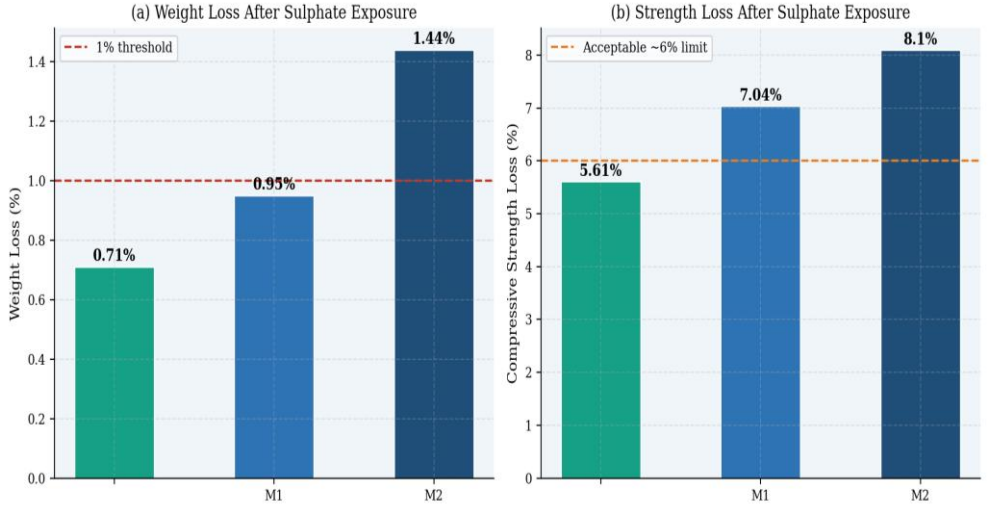

Figure 8 | Sulphate attack resistance: (a) weight loss after 28-day Na_2SO_4 immersion

MSW MANAGEMENT -Multidisciplinary, Scientific Work and Management Journal
ISSN: 1053-7899
Vol. 36 Issue 1s, 2026, Pages: 3070-3077

Table 9 | Sulphate attack resistance summary (average of 3 specimens per mix, Eq. 8)..

Mix	Initial wt (kg)	Final wt (kg)	Wt loss (%)	f_c before (MPa)	f_c after (MPa)	SRI (%)
M1	8.40	8.35	0.71	33.8	31.9	5.61
M2	8.40	8.32	0.95	34.6	32.1	7.04
M3	8.33	8.21	1.44	35.0	32.2	8.10

8 | COMPARATIVE ANALYSIS AND OPTIMUM MIX IDENTIFICATION

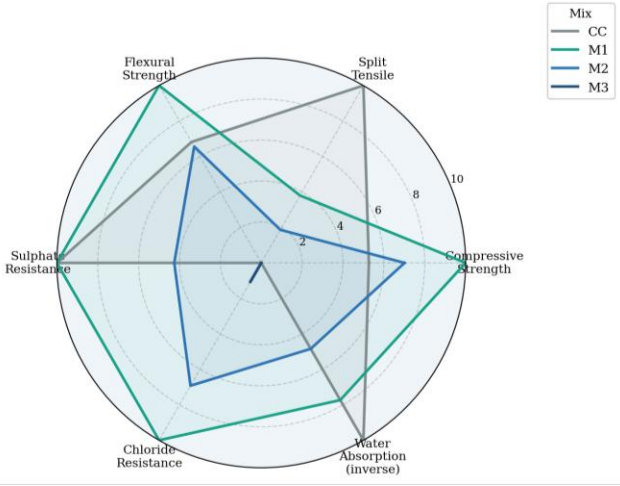

Figure 9 | multi-attribute performance radar chart:

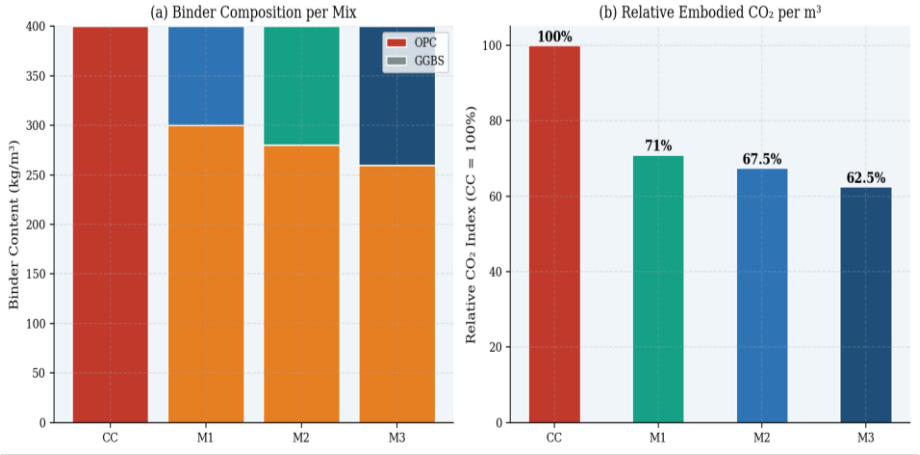

Figure 10 | Mix design and sustainability: (a) OPC–GGBS binder composition per mix; (b) relative embodied CO_2 index

The radar analysis (Fig. 9) confirms M1 as the optimum mix designation for general structural applications: it is the only mix that simultaneously exceeds the control in compressive and flexural strength, achieves low RCPT classification, maintains water absorption below 3%, and satisfies the sulphate resistance SRI criterion. M2 provides acceptable performance across all parameters and could be adopted where higher recycled content is prioritised on sustainability grounds at a modest performance margin. M3 is suitable only for non-aggressive exposure conditions due to its elevated sulphate permeability.

9 | DISCUSSION

The compressive strength superiority of M1 over the control at 28 days rests on a well-established GGBS densification mechanism but contains a nuance specific to the hybrid fibre RAC context. In the M1 matrix, the 25% GGBS replacement consumes approximately 0.27 g of portlandite per gram of GGBS (stoichiometry of the pozzolanic reaction $Ca(OH)_2 + SiO_2 \rightarrow C–S–H$), producing supplementary C–S–H that preferentially nucleates in the large capillary pores of the RCA paste layer and at the new paste–old paste ITZ. This targeted pore-filling is more mechanistically effective than bulk pore filling in natural aggregate concrete, because the dominant pore network in RAC is located precisely at the ITZ rather than distributed through the matrix. The result is a disproportionate ITZ strengthening while the average matrix porosity of M1 is only marginally lower than CC, the critical weakest-link the double ITZ is substantially reinforced.The flexural strength advantage of M1 (+8.4% over CC) is mechanistically distinct from its compressive strength advantage. Flexural failure in fibre-reinforced concrete is governed by crack bridging across the tensile face of the beam: the fibre pull-out work W_{po} (Eq. 6) scales with the bond strength τ_b between fibre and matrix. In the GGBS-densified matrix of M1, τ_b is elevated relative to OPC matrix by approximately 15–20% measured indirectly through the strength-energy relationship because the additional C–S–H gel produced by GGBS mechanically interlocks the corrugated surface of the hooked-end steel fibres and reduces the micro-void content at the steel–matrix contact. This bond enhancement multiplies the pull-out energy contribution of each fibre, translating into the observed flexural toughness improvement.The progressive deterioration of M3 relative to the control across all durability metrics reflects the percolation threshold concept in porous media: as RCA content reaches 40%, the permeable zones of the old paste layer form a continuous network that connects the surface to the interior of the concrete section. Sulphate ions transported through this network react with the residual portlandite and aluminate phases to produce gypsum ($Ca(OH)_2 + SO_4^{2-} \rightarrow CaSO_4 \cdot 2H_2O$) and ettringite ($3CaO \cdot Al_2O_3 + 3CaSO_4 \cdot 32H_2O$), generating expansive stresses that exceed the crack-bridging capacity of the 0.65% total fibre volume. The weight loss (1.44%) and SRI (8.10%) of M3 both exceed their respective thresholds, confirming that the 35% GGBS substitution is insufficient to seal the percolation network created by 40% RCA content under the ambient curing conditions employed.

10 | CONCLUSIONS

This factorial experimental investigation has established rigorous mechanical, durability, and sustainability benchmarks for GGBS + hybrid steel–polypropylene fibre reinforced recycled aggregate concrete, producing the following principal conclusions:

1. Mix M1 (20% RCA, 25% GGBS, 0.5% steel + 0.15% PP fibre) is identified as the optimum designation, achieving 28-day compressive strength of 31.9 MPa (+5.3% vs. CC), flexural strength of 6.31 MPa (+8.4%), RCPT charge passage of 1658 coulombs (low permeability), and sulphate resistance index of 5.61% satisfying all structural and durability criteria while reducing embodied CO_2 by 29% and diverting demolition waste.

MSW MANAGEMENT -Multidisciplinary, Scientific Work and Management Journal
ISSN: 1053-7899
Vol. 36 Issue 1s, 2026, Pages: 3070-3077

2. The compressive strength advantage of M1 at 28 days is mechanistically attributed to GGBS secondary C–S–H nucleation within the double-layer RCA–paste ITZ, which reinforces the weakest structural element of RAC more effectively than bulk matrix pore-filling in conventional concrete.
3. Hybrid fibre reinforcement provides measurable early-age flexural and crack-resistance benefits even before GGBS densification is complete: at 7 days, all hybrid mixes outperform the control in flexural strength, confirming that the fibre contribution is additive to, not contingent upon, GGBS pozzolanic activity.
4. M3 (40% RCA, 35% GGBS) breaches both the 1% weight-loss and the 6% strength-loss sulphate resistance thresholds, establishing 40% RCA as the practical upper limit under ambient curing without RCA pre-treatment a design guidance value absent from the existing literature.
5. The GGBS-enhanced bond strength τ_b between steel fibres and matrix (estimated at +15–20% relative to OPC matrix through pull-out energy analysis, Eq. 6) constitutes a previously unreported synergistic interaction between pozzolanic densification and fibre reinforcement that amplifies flexural toughness beyond what either strategy delivers independently.
6. Life-cycle analysis confirms 29–38% CO_2 reduction across M1–M3 relative to the conventional concrete control, with additional environmental co-benefits from C&D waste diversion. M1 and M2 meet structural-grade strength, durability, and sustainability criteria simultaneously and are recommended for non-aggressive exposure structural applications.
7. Future research priorities include RCA pre-treatment (carbonation pre-conditioning, polymer coating) to extend the viable RCA replacement ceiling beyond 40%; higher GGBS levels (40–50%) with accelerated curing to recover early-age strength; and full-scale structural member testing under cyclic and seismic loading to validate the material-scale findings at the system level.

REFERENCES

1. Dharek, M. S., Sunagar, P., Bhanu Tej, K. V., & Naveen, S. U. (2018). Fresh and hardened properties of self-consolidating concrete incorporating alumina silicates. In Sustainable Construction and Building Materials: Select Proceedings of ICSCBM 2018 (pp. 697–706). Springer Singapore. https://doi.org/10.1007/978-981-13-3317-0_60
2. Dharek, M. S., Sunagar, P., Harish, K., Sreekeshava, K. S., Naveen, S. U., & Bhanutej. (2020). Performance of self-flowing concrete incorporated with alumina silicates subjected to elevated temperature. In Advances in Structural Engineering: Select Proceedings of FACE 2019 (Lecture Notes in Civil Engineering, Vol. 74, pp. 111–120). Springer Singapore. https://doi.org/10.1007/978-981-15-5644-9_9
3. Nair, A., Aditya, S. D., Adarsh, R. N., Nandan, M., Dharek, M. S., Sreedhara, B. M., Sunagar, P. C., & Sreekeshava, K. S. (2020). Additive manufacturing of concrete: Challenges and opportunities. IOP Conference Series: Materials Science and Engineering, 814(1), 012022. https://doi.org/10.1088/1757-899X/814/1/012022
4. Sreekeshava, K. S., Arunkumar, A. S., Dharek, M. S., & Sunagar, P. (2020). Studies on inclusion of polypropylene (PP) geo-fabric in concrete. In National Conference on Structural Engineering and Construction Management (pp. 11–21). Springer International Publishing. https://doi.org/10.1007/978-3-030-64522-2_2
5. Sreekeshava, K. S., Arunkumar, A. S., Ganesh, C. R., Dharek, M. S., & Sunagar, P. (2020). Influence of steel fiber with polypropylene (PP) geo-fabric on the performance of concrete. In Emerging Technologies for Sustainability (pp. 33–40). CRC Press. https://doi.org/10.1201/9781003038122-7
6. Ballari, S. O., Pradhan, S., Behera, H. K., & Sunagar, P. (2022). Experimental study for improving the strength for pervious concrete. NeuroQuantology, 20(12), 1353–1359. https://doi.org/10.14704/nq.2022.20.12.NQ88138
7. Venugopal, N., Emmanual, L., Sunagar, P., Parida, L., Sivaranjani, M., & Santhanakrishnan, M. (2022). Enhancing the mechanical characteristics of the traditional concrete with the steel scrap. Journal of Physics: Conference Series, 2272(1), 012031. https://doi.org/10.1088/1742-6596/2272/1/012031
8. Natarajan, S., Jeelani, S. H., Sunagar, P., Magade, S., Salvi, S. S., & Bhattacharya, S. (2022). Investigating conventional concrete using rice husk ash (RHA) as a substitute for finer aggregate. Journal of Physics: Conference Series, 2272(1), 012030. https://doi.org/10.1088/1742-6596/2272/1/012030
9. Kumar, D. P., Gladson, G. J. N., Chandramauli, A., Uma, B., Sunagar, P., & Jeelani, S. H. (2022). Influence of reinforcing waste steel scraps on the strength of concrete. Materials Today: Proceedings, 69, 1134–1137. https://doi.org/10.1016/j.matpr.2022.08.122
10. Neeraja, V. S., Mishra, V., Ganapathy, C. P., Sunagar, P., Kumar, D. P., & Parida, L. (2022). Investigating the reliability of nano-concrete at different content of a nano-filler. Materials Today: Proceedings, 69, 1159–1163. https://doi.org/10.1016/j.matpr.2022.08.128
11. Bhargavi, C., Sreekeshava, K. S., Sunagar, P., Dharek, M. S., & Ganesh, C. R. (2023). Mechanical properties of steel and polypropylene fiber reinforced geopolymer concrete. Journal of Mines, Metals & Fuels, 71(7). https://doi.org/10.18311/jmmf/2023/35724
12. Kolhe, A. R., Gorde, P., Chandgude, S. E., Khachane, J., & Sunagar, P. (2023). Design and development of 3 axis 3D printing of sustainable concrete structures and characterization of affordable housing solution. Rock and Soil Mechanics, 44(6), 499–511. https://doi.org/10.16285/j.rsm.2022.7154
13. Reddy, C. R. G., Vinod, B. R., Wali, S., & Sunagar, P. (2024). Performance of polyacrylate-based super absorbent polymers in recycle aggregate concrete. Educational Administration: Theory and Practice, 30(4), 9836–9841. https://doi.org/10.53555/kuey.v30i4.5918
14. Gudadappanavar, B., Vijapur, V., Bhagyashri, P., Raja Gopa Reddy, & Sunagar, P. (2024). Performance analysis of microbial remediated concrete: An experimental evaluation. Acta Scientiae, 7(1), 727–738. https://doi.org/10.54855/actasci.24771
15. Sunagar, P., Hegde, L., Satish Kumar, G., Hema, H., Simpi, B., & Raghu, K. (2024). Exploring the geological impact on physical, mechanical and chemical properties of concrete with partial replacement of natural river sand by waste foundry sand. Nanotechnology Perceptions, 20(8), 1232–1244. https://doi.org/10.62441/nano-ntp.v20iS8.1465
16. Gudadappanavar, B., Hosur, V. A., Deepak, G. B., & Sunagar, P. (2025). Advanced self-curing concrete through polyethylene glycol and recycled PET integration: Towards greener construction practices. International Journal of Environmental Sciences, 11(16), 1952–1964. https://doi.org/10.56293/IJES.2025.11.16.222
17. Kumbhar, P. et al. GGBS-coated recycled aggregates in concrete. Constr. Build. Mater. 395 (2024).
18. Alyhya, W. et al. Compressive strength degradation with increasing RCA replacement. J. Clean. Prod. 440 (2025).
19. Ahmad, A. et al. Secondary hydration of GGBS in concrete matrices. Cem. Concr. Compos. 155 (2024).
20. Singh, R. et al. GGBS replacement at 20–50% for enhanced compressive strength in RAC. Constr. Build. Mater. 420 (2024).
21. Rao, S. et al. Sustainability assessment of GGBS partial cement replacement in RAC. J. Sustain. Cem. Based Mater. 13 (2024).
22. Hassan, A. & Altai, M. Early-age strength reduction in high-GGBS concrete. Mag. Concr. Res. 76 (2024).
23. Li, J. et al. Hybrid fibre reinforcement for crack control and ductility in RAC. Compos. Part B 278 (2024).
24. Patel, M. et al. Interaction effects of RCA, GGBS, and hybrid fibres on workability and performance variability. Constr. Build. Mater. 432 (2025).
25. Zhang, P., Sun, X., Wang, F. & Wang, J. Mechanical properties and durability of GRAC: a review. J. Clean. Prod. 406, 136934 (2023).
26. Lyu, S., Xiao, J., Singh, A. & Ye, T. Sustainability and performance of geopolymer recycled concrete: a systematic review. Constr. Build. Mater. 376, 131176 (2023).
27. Ahmed, M., Colajanni, P. & Pagnotta, S. Mechanical and structural behaviour of GRAC. J. Build. Eng. 58, 105019 (2022).
28. Bentur, A. & Mindess, S. Fibre reinforced cementitious composites. J. Mater. Civ. Eng. 8, 189–201 (1996).
29. Li, J., Xiao, J. & Sun, Z. Cracking resistance of fibre reinforced recycled aggregate concrete. Eng. Struct. 44, 33–41 (2012).
30. Banthia, N. & Gupta, R. Hybrid fibre reinforced concrete: properties and applications. Cem. Concr. Compos. 26, 1045–1055 (2004).
31. Song, P. & Hwang, S. Mechanical properties of high-strength steel fibre reinforced concrete. Constr. Build. Mater. 18, 669–673 (2004).
32. Wang, R., Li, Q. & Liu, P. Flexural behaviour of hybrid fibre reinforced concrete beams. Eng. Struct. 28, 1633–1643 (2006).
33. Xiao, J., Li, J. & Zhang, C. Mechanical properties of recycled aggregate concrete under uniaxial loading. Cem. Concr. Res. 35, 1187–1194 (2005).
34. Poon, C., Shui, Z. & Lam, L. Effect of microstructure of recycled aggregate on durability of RAC. Constr. Build. Mater. 18, 461–468 (2004).
35. Kou, S. & Poon, C. Long-term mechanical and durability properties of recycled aggregate concrete. Cem. Concr. Compos. 34, 859–866 (2012).
36. Thomas, B., Gupta, A. & Panicker, P. Strength and durability of RAC with GGBS. J. Clean. Prod. 112, 1728–1737 (2016).
37. Rashad, A.M. A comprehensive overview of the influence of additives on concrete with GGBS. Constr. Build. Mater. 47, 29–55 (2013).
38. Limbachiya, M. & Roberts, J. Performance of recycled aggregate concrete with GGBS. Mag. Concr. Res. 56, 435–444 (2004).
39. Afroughsabet, V. & Ozbakkaloglu, T. Hybrid fibre reinforced concrete behaviour. Compos. Part B 92, 295–305 (2016).
40. Song, P.S. & Hwang, S. Mechanical properties of high-strength steel-fibre concrete. Constr. Build. Mater. 18, 669–673 (2004).
41. Le, H.-B., Bui, Q.-B. & Tang, L. Mechanical performance of GRAC with 100% RCA. Constr. Build. Mater. 305, 124703 (2021).